Journal of Electroanalytical Chemistry 785 (2017) 58–64

Contents lists available at ScienceDirect

Journal of Electroanalytical Chemistry

journal homepage: www.elsevier.com/locate/jelechem

The effect of oxidation state of metal on hydrogen production electro-catalyzed by nickel complexes supported by maleonitriledithiolate ligand

Chen-Neng Lin [a], Dan Xue [a], Yi-Hang Zhou [b], Shu-Zhong Zhan [a,*], Chun-Lin Ni [b,*]

[a] College of Chemistry & Chemical Engineering, South China University of Technology, Guangzhou 510640, China
[b] College of Materials and Energy, Institute of Biomaterial, South China Agricultural University, Guangzhou 510642, China

ARTICLE INFO

Article history:
Received 10 July 2016
Received in revised form 24 November 2016
Accepted 7 December 2016
Available online xxxx

Keywords:
Nickel(II) and nickel(III) complexes
Electrocatalysts
Proton and water reduction
Hydrogen evolution

ABSTRACT

Two molecular electro-catalysts based on nickel complexes, $[Ni(mnt)_2]^{n-}$ (n = 2 (**1**) and 1 (**2**)) are formed by the reactions of $NiCl_2 \cdot 6H_2O$, $Na_2(mnt)$ and $[BzPyN(CH_3)_2]Br$ or $[4\text{-}ClBzPyN(CH_3)_2]Br$ ($BzPyN(CH_3)_2$ = 1-benzyl-4-(dimethylamino)pyridinium, mnt = 2.2-dicyanoethylene-1.1-dithiolate, and $4\text{-}ClBzPyN(CH_3)_2$ = 4-Cl-benzyl-4-dimethylaminopyridinium). Electrochemical investigations show **1** and **2** can electrocatalyze hydrogen generation both from acetic acid and aqueous buffer solution. And complexes **1** and **2** afford a turnover frequency (TOF) of 282.95 and 504.25 mol of hydrogen per mole of catalyst per hour at an overpotential (OP) of 0.848 V from a neutral buffer, respectively, indicating that the nickel(III) complex constitutes the better active catalyst than the nickel(II) species.

1. Introduction

In order to avoid energy crisis, people are developing new systems to get new energy. And hydrogen is of particular interest as a secondary energy carrier, its generation from water is a current topic of intensive research [1,2]. In particular, electro-catalytic method for hydrogen generation from organic acid or water have been explored as cost-effective ways of producing a carbon-neutral fuel. However, one of the key challenges for hydrogen generation by proton or water reduction is the development of efficient catalysts with low overpotential, good stability, and high turnover rate [3,4]. Therefore, a great deal of research efforts have been devoted to the development of effective catalysts based on transition metal complexes, such as manganese [5], nickel [6–9], cobalt [10–12] and copper [13–15] for the reduction of proton or water to form H_2. There are several reports about that the donor type and electronic properties of the ligands play vital roles in determining the structure and reactivity of the corresponding metal complexes [16–18]. However, few studies on catalytic properties by metal complexes with varying oxidation states. In this paper, we report the investigation on two molecular electrocatalysts based on nickel complexes, $[Ni(mnt)_2]^{n-}$ (n = 1 or 2) with different oxidation states. Both nickel complexes exhibit electrocatalytic activity for hydrogen generation from acetic acid and aqueous buffer.

2. Experimental

2.1. Materials and physical measurements

2-Chlorobenzyl bromide, 3-chlorobenzyl bromide, 4-chlorobenzyl bromide and 4-dimethylaminopyridine were purchased from Aldrich and were used without further purification. 1-(4′-chlorobenzyl)-4-dimethylaminopyridinium bromide ($[4ClBzPyN(CH_3)_2]Br$) and disodium maleonitriledithiolate (Na_2mnt) were synthesized following the literature procedures [19,20]. $[BzPyN(CH_3)_2]_2[Ni(mnt)_2]$ **1** and $[4\text{-}ClBzPyN(CH_3)_2][Ni(mnt)_2]$ **2** (mnt^{2-} = maleonitriledithiolate) were prepared according to the reported methods [21,22]. Elemental analyses for C, H, and N were obtained on a Perkin-Elmer analyzer model 240. UV–Vis spectra were measured on a Hitachi U-3010 spectrometer. ESI-MS experiments were performed on a Bruker Daltonics Esquire 3000 Spectrometer by introducing samples directly into the ESI source using a syringe pump. X-ray photoelectron analysis were carried out by ESCALAB 250 Xi X-photoelectron spectroscopy with monochromatic Al Kα (1486.6 eV) X-ray sources. Electrochemical measurements were conducted on a CHI-660E electrochemical analyzer under N_2 using a three-electrode cell in which a glassy carbon electrode was the working electrode, an $Ag/AgNO_3$ (organic media) or a saturated Ag/AgCl (aqueous media) electrode was the reference electrode, and platinum wire was the auxiliary electrode. In organic media, a ferrocene/ferrocenium (1+) couple was used as an internal standard, and 0.10 mol L^{-1} $[(n\text{-}Bu)_4N]ClO_4$ was used as the supporting electrolyte. Controlled-potential electrolysis (CPE) in aqueous media was conducted using an air-tight

* Corresponding authors.
E-mail address: shzhzhan@scut.edu.cn (S.-Z. Zhan).

http://dx.doi.org/10.1016/j.jelechem.2016.12.011
1572-6657/

glass double compartment cell separated by a glass frit. The working compartment was fitted with a glassy carbon plate and an Ag/AgCl reference electrode. The auxiliary compartment was fitted with a Pt gauze electrode. The working compartment was filled with 0.050 L of 0.25 mol L^{-1} phosphate buffer, while the auxiliary compartment was filled with 0.035 L phosphate buffer solution. After adding **1** or **2**, cyclic voltammograms were recorded. After electrolysis, a 5.0×10^{-4} L aliquot of the headspace was removed and replaced with 5.0×10^{-4} L of CH_4. The headspace sample was injected into the gas chromatograph (GC). GC experiments were carried out with an Agilent Technologies 7890A gas chromatography instrument. Gaussian 09 data package [23] were used to complete all theoretical calculations. N and C atoms were calculated by using M06-2X/6-311++G(2df, 2p), and S atoms were calculated by using M06-2X/6-311++G(3df, 3pd). AUG-cc-pVTZ was used to calculate Ni atoms. Polarized continuum model (PCM) [24], radii and non-electrostatic model (SMD) [25] were used to estimate the energy in acetonitrile. The relation of gas and liquid phase Gibbs free energy follows $\Delta G_{(aq)} \approx \Delta G_{(gas)} + \Delta(\Delta G_{(sol)})$. $\Delta G_{(aq)}$ and $\Delta G_{(gas)}$ stand for gas and liquid phase Gibbs free energy, respectively. $\Delta(\Delta G_{(sol)})$ indicates the variable of the Gibbs free energy by solvation.

3. Results and discussion

3.1. General characterization

Experimentally, the direct combination of 1:2:2 mol equiv. of $NiCl_2 \cdot 6H_2O$, Na_2mnt and 1-benzyl-4-(dimethylamino)pyridinium bromide affords a nickel(II) complex, $[BzPyN(CH_3)_2]_2[Ni(mnt)_2]$ **1**. In the presence of I_2, the reaction of $NiCl_2 \cdot 6H_2O$, Na_2mnt and 1-(4′-chlorobenzyl)-4-dimethylaminopyridinium bromide at a mole ratio of 1:2:1 provides a nickel(III) complex, $[4\text{-}ClBzPyN(CH_3)_2][Ni(mnt)_2]$ **2** (Scheme 1). These results are also in agreement with the X-ray photoelectron spectroscopy (XPS) analysis (Figs. S1–S2). As shown in Fig. S1, XPS spectrum of complex **1** shows one peak at 854.5 eV, which is assigned to Ni^{2+} $2p_{3/2}$, a typical characteristic of Ni(II) oxidation state. The Ni $2p_{3/2}$ region for complex **2** shows one peak at 855.3 eV (Fig. S2), which is assigned to Ni^{3+} $2p_{3/2}$, indicating that the oxidation state of nickel in complex **2** is +3. These are consistent with the results reported in the literature [26].

To test properties of complexes **1** and **2** in liquid, electronic spectra were measured in both organic and aqueous media. From Fig. S3, the UV/Vis spectrum of **1** in acetonitrile shows an absorption peak at 438 nm, which corresponds to a ligand-metal-charge-transition (LMCT) between the ligands and nickel ion. And complex **2** exhibits a LMCT at 478 nm. As shown in Fig. S4, in aqueous buffer at the pH range 2.0–11.0, the intensities of the absorption bands of complex **1** at 316 and 428 nm indeed changes, but the peak position does not move, suggesting there are new components appear under these conditions, such as $[H\text{-}Ni(mnt)_2]^-$ or $[HO\text{-}Ni(mnt)_2]^{3-}$. From Fig. S5, the intensities of the absorption bands of complex **2** at 289 and 375 nm also changes with varying pH values, indicating there are new components appear under these conditions.

In methanol, complex **1** exits the same state as that in solid. This is in agreement with the result from ESI-MS measurement which exhibits one ion at a mass-to-charge ratio (m/z) of 340.2737, with the mass and isotope distribution pattern corresponding to that of $[Ni^{II}(mnt)_2H]^-$ (Fig. S6). Similarly, in methanol, complex **2** exhibits one ion at a mass-to-charge ratio (m/z) of 340.2693, with the mass and isotope distribution pattern corresponding to that of $[Ni^{III}(mnt)_2H]$ (Fig. S7).

3.2. Linear scan voltammetry

To test if these two nickel complexes can act as electrocatalysts, first we used linear scan voltammetry (LSV) to investigate their electrochemical behaviors. As shown in Fig. 1a, the potential for reduction of **1** are the same as that of the back-ground (ca. −1.55 V versus Ag/AgCl), indicating that no proton is lost during the initial reduction. Similar to that of complex **1**, no proton is lost during the initial reduction for complex **2** (Fig. 1b). According to Fig. 1, the peak current increases continually with increasing complex **1** or **2** concentration from 0.0 to 4.08×10^{-4} mol L^{-1}, and no turning point is found, demonstrating

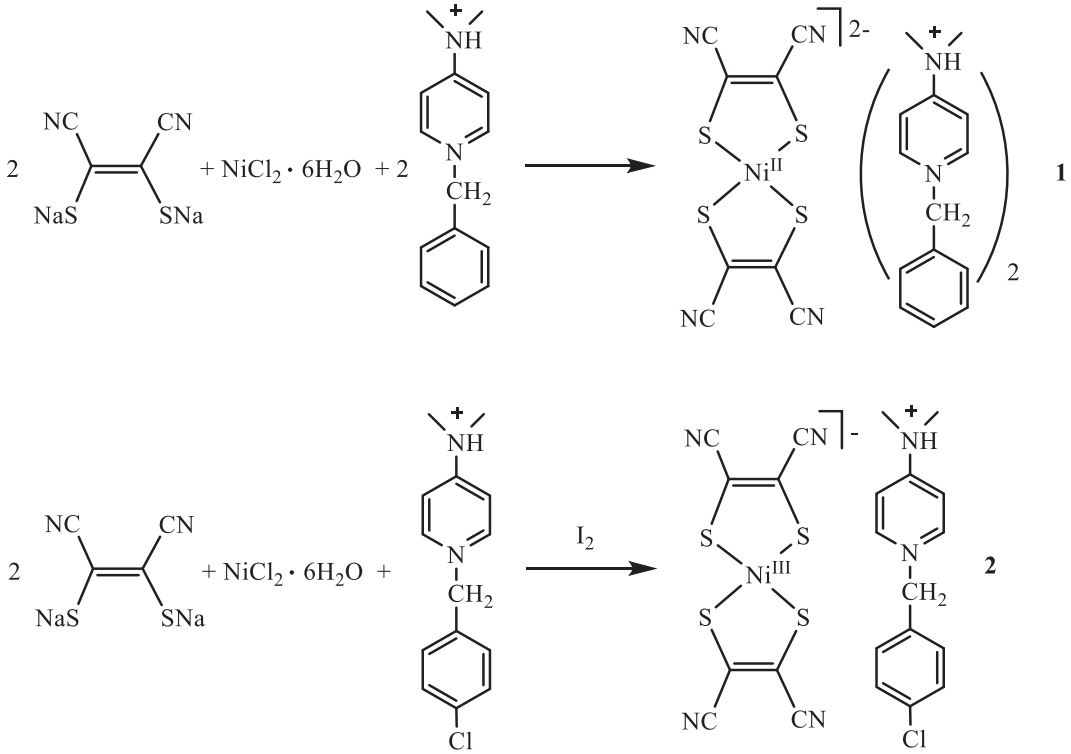

Scheme 1. Schematic representation of the synthesis of nickel complexes **1** and **2**.